JCTC Journal of Chemical Theory and Computation

Mechanism of Air Oxidation of the Fragrance Terpene Geraniol

Carina Bäcktorp,[†] Lina Hagvall,[‡] Anna Börje,[‡] Ann-Therese Karlberg,[‡] Per-Ola Norrby,*[,§] and Gunnar Nyman[†]

Department of Chemistry, Physical Chemistry, Göteborg University, SE-412 96 Göteborg, Sweden, Department of Chemistry, Dermatochemistry and Skin Allergy, Göteborg University, SE-412 96 Göteborg, Sweden, and Department of Chemistry, Organic Chemistry, Göteborg University, SE-412 96 Göteborg, Sweden

Received June 20, 2007

Abstract: The fragrance terpene geraniol autoxidizes upon air exposure and forms a mixture of oxidation products, some of which are skin sensitizers. Reactions of geraniol with O_2 have been studied with DFT (B3LYP) and the computational results compared to experimentally observed product ratios. The oxidation is initiated by hydrogen abstraction, forming an allylic radical which combines with an O_2 molecule to yield an intermediate peroxyl radical. In the subsequent step, geraniol differs from previously studied cases, in which the radical chain reaction is propagated through intermolecular hydrogen abstraction. The hydroxy-substituted allylic peroxyl radical prefers an intramolecular rearrangement, producing observable aldehydes and the hydroperoxyl radical, which in turn can propagate the radical reaction. Secondary oxidation products like epoxides and formates were also considered, and plausible reaction pathways for formation are proposed.

Introduction

Contact allergy, caused by skin-penetrating compounds able to react with macromolecules in the skin to form antigens, is one of the most common health problems in the industrialized world. In Western Europe, an estimated 10−15% of the normal population suffers from contact allergies that upon prolonged or repeated contact with the offending agent result in allergic contact dermatitis. Fragrance compounds commonly cause contact allergies. Fragrances are ubiquitous in our environment, and not only cosmetics and toiletries contain fragrance materials but almost all household and occupational products are scented. The allergens are not always the fragrance compounds themselves, but rather degradation products formed upon prolonged storage in contact with air, for example, in scented products.

As part of a long-term project of identifying compounds that are not allergenic themselves but can form allergenic compounds upon air exposure, it has been shown how some common fragrance terpenes form allergenic hydroperoxides and secondary oxidation products upon exposure to air. The oxidation products were isolated and identified, and their allergenic effects were determined experimentally.[1−4]

In the mechanism for autoxidation of the unsaturated terpene linalool (**1**, Figure 1), oxidation was found to occur by abstraction of an allylic hydrogen, followed by combination with O_2 and radical chain propagation to yield allylic hydroperoxides as primary oxidation products.[5]

A recent study investigated the bimolecular reaction between an alkene and triplet oxygen, requiring a spin-state change to reach the singlet products.[6] However, in general, the formation of hydroperoxides via autoxidation is believed[5] to proceed through a radical chain process according to the following steps:

$$\text{Initiation: } RH \rightarrow R\cdot \qquad \text{(step 1)}$$

$$\text{Propagation: } R\cdot + O_2 \rightarrow ROO\cdot \qquad \text{(step 2a)}$$

$$ROO\cdot + R'H \rightarrow ROOH + R'\cdot \qquad \text{(step 2b)}$$

$$\text{Termination } 2R'\cdot \rightarrow \text{nonradical products} \qquad \text{(step 3)}$$

* Corresponding author e-mail: pon@chem.gu.se.
[†] Department of Chemistry, Physical Chemistry.
[‡] Department of Chemistry, Dermatochemistry and Skin Allergy.
[§] Department of Chemistry, Organic Chemistry.

10.1021/ct7001495 CCC: $40.75
Published on Web 11/03/2007

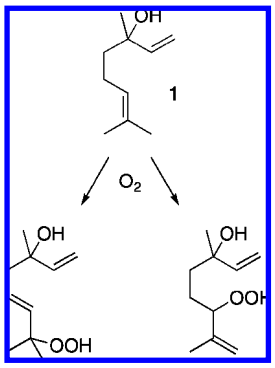

Figure 1. Linalool (**1**) and two hydroperoxides identified after air oxidation.

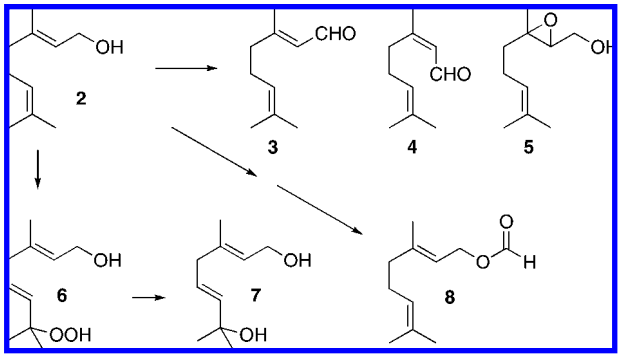

Figure 2. Geraniol (**2**) with identified air oxidation products.

Here 2R′• can be any combination of the radicals formed. We note that no step in the chain process requires a change of spin. The exothermic addition of oxygen to the radical, step 2a, is believed to occur without any barrier on the potential energy surface (i.e., it is diffusion-controlled, *vide infra*); hence, the rate and selectivity determining step of the propagation is the hydrogen atom abstraction, step 2b.

Geraniol (**2**, *trans*-3,7-dimethyl-2,6-octadiene-1-ol), an isomer of **1**, is an important fragrance terpene, widely used because of its fresh flowery odor. A recent investigation[7] of the air oxidation of geraniol (**2**, Figure 2) revealed that the reaction is substantially more complex than that of **1**, forming a mixture of products that include hydrogen peroxide, the aldehydes geranial (**3**) and neral (**4**), and epoxygeraniol (**5**), in addition to a hydroperoxide (**6**) related to those found in the linalool study,[4] and its secondary degradation product, the allylic alcohol **7**. Furthermore, the presence of geranyl formate (**8**) in the oxidation mixture must be rationalized by a postoxidation bimolecular transformation, since the additional carbon in the formate moiety has to come from another, degraded geraniol molecule. Studies of the skin-sensitizing potency according to the local lymph node assay in mice showed that air-exposed geraniol as well as several of the isolated oxidation products have a sensitizing potency significantly higher than that of pure geraniol, demonstrating the need for an increased understanding of the oxidation of fragrance terpenes.[7]

In an earlier investigation of geraniol, it could be concluded that the most easily abstracted allylic hydrogen is the one α to the hydroxyl, leading to the preferential formation of radical **A** (Figure 3).[7]

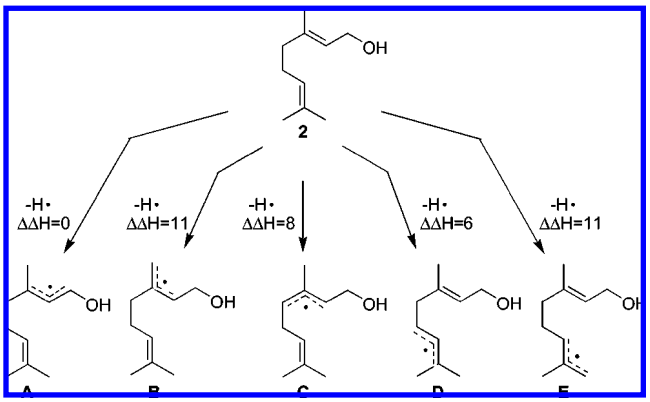

Figure 3. Illustration of five radicals that can be formed by hydrogen abstraction from geraniol. Enthalpy changes (in kcal mol^{-1}) for forming the various radicals are given relative to radical **A**.

Radical **D** is less stable than **A**, but some products derived from radical **D** were still observed (**6** and **7**, Figure 2). The three other radicals, **B**, **C**, and **E**, are even higher in energy, and indeed no oxidation products derived from any of these could be identified.[7] The formation of products from **D** is analogous to the previously investigated oxidation of linalool (**1**)[3−5] and will not be further discussed here. Instead, we will concentrate on the possible further reactions of radical **A**.

In this work, we report our theoretical investigation of the mechanism of oxidation of geraniol (**2**). In the current work, we focus upon the primary oxidation, which follows a radical chain process, forming the primary oxidation products in the presence of triplet oxygen. Secondary oxidation products are then formed in closed-shell processes for which there are ample precedents in the literature.

Computational Methods

All calculations were performed using unrestricted density functional theory (DFT) with the B3LYP functional[8] as implemented in Gaussian 03.[9] We utilized two different basis sets, optimizing all structures first with 6-31G(d,p), and then using the larger 6-311+G(2d,p) basis set. Harmonic vibrational frequencies were obtained for all structures (and both basis sets) in order to ensure the nature of the stationary points (saddle point or minimum), and also to estimate the thermodynamic contribution to the enthalpy and free energy at $T = 298$ K. Energies are reported as enthalpies at 0 K and at 298 K, and free energies at 298 K.

Results and Discussion

In the investigation of the formation and further reactions of radical **A** (Figure 3), we have chosen to use a smaller and less flexible molecule, 3-methyl-2-buten-1-ol (**9,** Figure 4), as the model for geraniol (**2**). This model includes all the features of **2** necessary for reproducing the stability of **A**, that is, the trisubstituted alkene and the allylic hydroxy functionality, but excludes the conformationally flexible isoprenoid moiety that is expected to stay constant in all investigated reactions. Depending on the conformation of the alcohol in the hydrogen abstraction step, two radicals

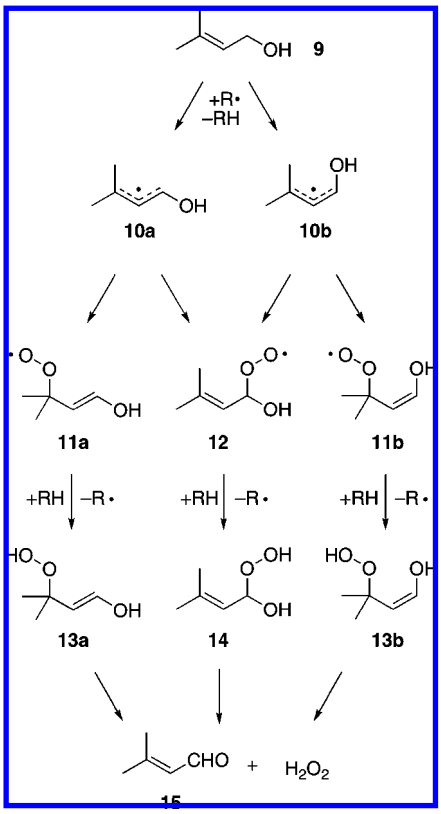

Figure 4. Propagation steps using the geraniol model **9**.

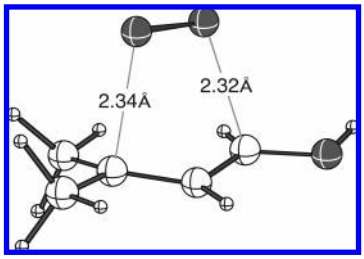

Figure 5. B3LYP/6-311+G(2d,p) TS for direct interconversion between **11a** and **12**.

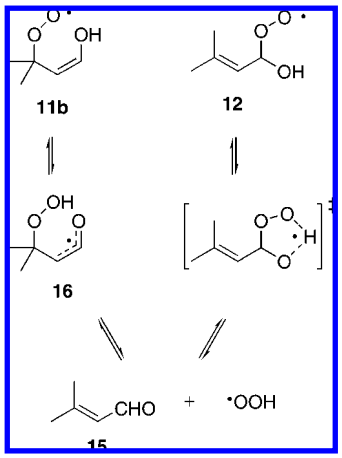

Figure 6. Alternative fragmentation paths for peroxyl radicals **11b** and **12**.

can be formed, **10a** and **10b** (Figure 4). For steric reasons, we expect the trans form, **10a**, to dominate, but both forms, and their potential interconversion pathways, have been included in the study.

Table 1. Calculated Standard Enthalpy Changes and Standard Gibbs Free Energy Changes in kcal mol^{-1} for the Reactions in Figure 4

	6-31G(d,p)			6-311+G(2d,p)		
	ΔH_0°	ΔH_{298}°	ΔG_{298}°	ΔH_0°	ΔH_{298}°	ΔG_{298}°
R• + O_2 → ROO• (step 2a)						
10a + O_2 → 11a	−16	−14	−2	−12	−13	0
10a + O_2 → 12	−21	−18	−7	−16	−17	−5
10b + O_2→ 11b	−23	−20	−7	−16	−17	−4
10b + O_2 → 12	−22	−20	−8	−17	−18	−7
ROO• + RH → ROOH + R• (step 2b)						
11a → 13a	−2	−3	−3	−4	−3	−4
12 → 14	−2	−3	−4	−5	−4	−6
11b → 13b	0	0	−1	−2	−1	−3
ROOH → aldehyde + H_2O_2						
13a → 15 + H_2O_2	5	3	−10	−1	0	−13
14 → 15 + H_2O_2	10	8	−4	4	5	−7
13b → 15 + H_2O_2	9	6	−8	0	1	−13

Table 2. Calculated Activation Energies, in kcal mol^{-1}

	6-31G(d,p)			6-311+G(2d,p)		
TS	ΔH_0°	ΔH_{298}°	ΔG_{298}°	ΔH_0°	ΔH_{298}°	ΔG_{298}°
11b → 16	6	5	6	6	6	7
12 → 15	3	3	3	4	4	4
11a → 12	10	10	10	9	9	9
11b → 12	17	17	15	15	15	16

No transition states (TSs) could be found for the first propagation step, the combination of radicals **10a** and **10b** with O_2. To verify that the addition is indeed barrier-less, we performed a geometry optimization starting with an O_2 molecule positioned perpendicular to the π-face of radical **10a**, with the closest oxygen−carbon distance set to 3 Å. In this optimization, the trust radius was strongly reduced, to 0.05 b, to ensure that the optimization sequence did not accidentally skip over a low barrier. Each step of the optimization was inspected, verifying that the steps were small and the energy decrease monotonous. The optimization proceeded as expected, and yielded structure **12**, showing that the addition can occur without an energy barrier.

The addition products **11** and **12** can potentially equilibrate by reverting to free O_2 and allylic radicals **10**. However, a direct [2,3] shift is also possible and was found to have an activation energy lower than that required for the dissociation of O_2. The transition state for direct conversion between **11a** and **12** is depicted in Figure 5. As can be seen, the TS is very symmetric, with forming and breaking C−O bonds of almost equal length. Interestingly enough, the TS structure is also very similar to one of the intermediate points in the slow optimization used to verify the barrier-less nature of the O_2 addition, indicating that it is also a potential branching point for the O_2 addition reaction.

In the last propagation step, peroxyl radicals **11**/**12** abstract a hydrogen from another species in solution, forming a new radical and the hydroperoxy species **13** and **14**. Each of these are expected to be in equilibrium with aldehyde **15** and hydrogen peroxide, which has also been detected in the

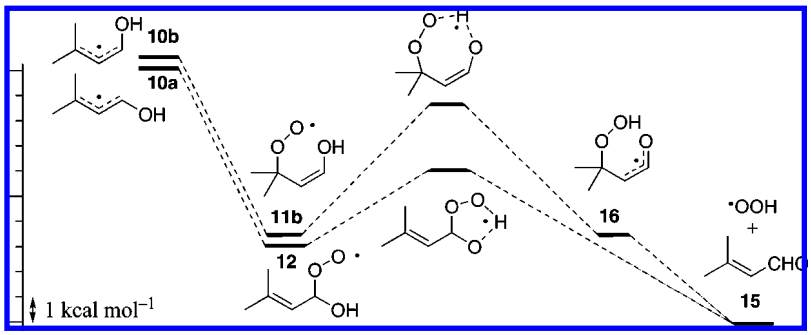

Figure 7. Free energy surface for the fragmentations depicted in Figure 6.

autoxidation sample. The calculated reaction energies and barriers for these steps are shown in Tables 1 and 2, respectively.

Analyzing first the effect of the two different basis sets, we can see that there are numerical differences, but that the qualitative picture is the same in both cases. Moreover, the change follows the expected trend. The basis superposition error (BSSE), which can be significant with smaller basis sets, will favor association, since a more compact arrangement of atoms allows the virtual orbitals from one fragment to fill out deficiencies in the orbital description of the neighboring fragment. Thus, with the larger basis set, the reaction between O_2 and allyl radicals becomes less exothermic, the proton-transfer steps are virtually unaffected, and the dissociation steps become more exothermic. We also want to point out that the BSSE to some extent compensates for an error in B3LYP, namely, the lack of proper treatment of dispersion forces. We are not aware of a full investigation of the relative magnitude of these effects, but in our experience with similar methods, a modest basis set frequently gives better agreement with experiments than the more extensive one. To conclude, we cannot be certain which of the two sets of data is in best agreement with experimental values, but it is reassuring that both sets give the same qualitative results. Since this is the case, we will perform additional calculations using the cheaper of the two methods, B3LYP/6-31G(d,p).

Looking at the two propagation steps, the initial combination of the allylic radical with O_2 (step 2a) occurs without a barrier on the potential energy surface (*vide supra*). For step 2b, the abstraction of a hydrogen atom from another molecule in solution forming hydroperoxides, we have investigated a model peroxyl radical, $CH_3OO\bullet$, reacting with the geraniol model **9** to form **10**, at the B3LYP/6-31G(d,p) level. For this step, we find an enthalpy of activation of 7 kcal mol^{-1}, and a free energy of activation of 18 kcal mol^{-1}. Thus, the reversion of step 2a, which is endergonic by 0−8 kcal mol^{-1},[10] is competitive with propagation. Peroxyl radical **11a** has no alternative forward reaction and may either revert to **10a** or isomerize to **12** to a significant extent. On the other hand, **11b** and **12** can follow alternative fragmentation paths due to the spatial proximity of the hydroxy group (Figure 6), in a heteroatom analogy to the known fragmentation of the ethylperoxyl radical.[11] As seen in the corresponding free energy surface, Figure 7, the intramolecular hydrogen transfer in **11b** to produce peroxy enolyl radical **16** is virtually isoergonic, with a moderate barrier. Intermediate **16** can then

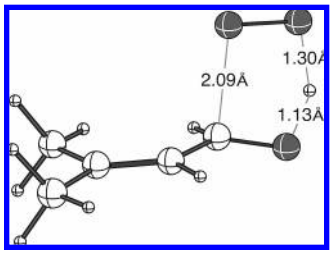

Figure 8. B3LYP/6-311+G(2d,p) TS for fragmentation of **12** to **15**.

eliminate a hydroperoxyl radical in an exergonic process, to form aldehyde **15**. For the hydroxy-substituted peroxyl radical **12**, the intramolecular hydrogen transfer and elimination are concerted, forming the hydroperoxyl radical and free aldehyde with a very low barrier (Figure 8).

Overall, fragmentation via **12** and intramolecular elimination is the preferred path, but as can be seen in Figure 7 and Table 2, when formed, peroxyl radical **11b** will prefer elimination via **16** over reversion to allylic radical **10** or isomerization to **12**.

In the full system starting from geraniol (**2**), we must also consider cis/trans isomerization, giving neral (**4**) in addition to geranial (**3**). In Figure 9, we have summarized the expected pathways and indicated intermediates where isomerization around the former double bond is feasible. For one peroxyl radical where no intramolecular hydrogen abstraction is possible (corresponding to **11a** in Figure 4), an equilibrium back to free O_2 and the allylic radical or a [2,3] shift is expected. Dotted arrows indicate intermolecular hydrogen abstraction followed by closed-shell fragmentation, as outlined in Figure 4. This process is expected to be disfavored compared with reversal and branching to a pathway allowing intramolecular hydrogen abstraction and fragmentation.

The hydroperoxyl radical produced by the fragmentations depicted in Figures 6 and 9 can participate in the radical chain propagation by abstracting a hydrogen atom from a molecule of geraniol (**2**). However, the reactive hydroperoxyl radical can also add to the double bond of geraniol, as shown for the model compound **9** in Figure 10. The addition is somewhat endergonic, but the subsequent ring closure to epoxy alcohol **17** is strongly exergonic. The liberated hydroxyl radical is highly reactive and will propagate the radical chain process by the abstraction of a hydrogen atom from a molecule of geraniol. Epoxygeraniol (**5**, corresponding to model compound **17**) has been detected in the autoxidation mixture.[7]

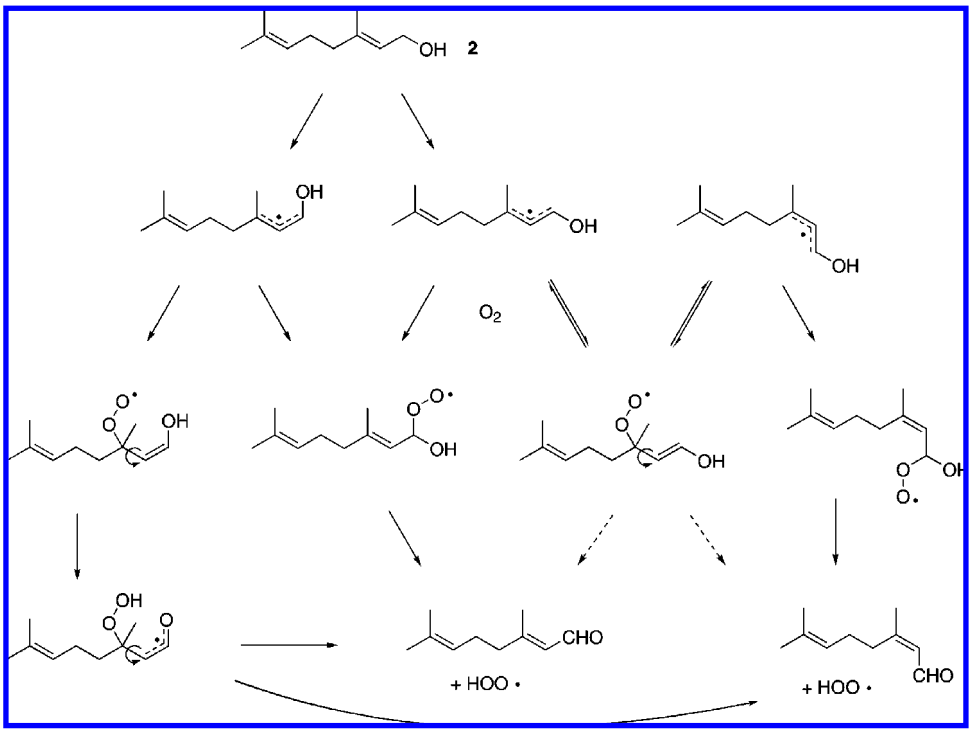

Figure 9. Expected open-shell autoxidation pathways starting from geraniol, **2**.

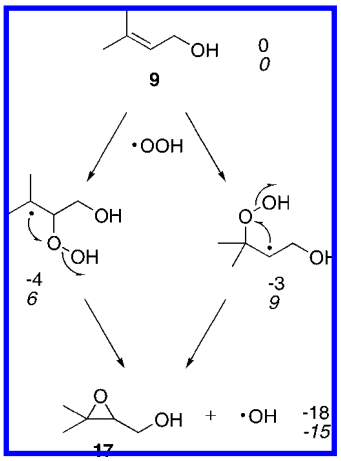

Figure 10. Epoxidation of geraniol model **9** by hydroperoxyl radical, with enthalpies and free energies (both at 298 K, the latter in italic) for all species.

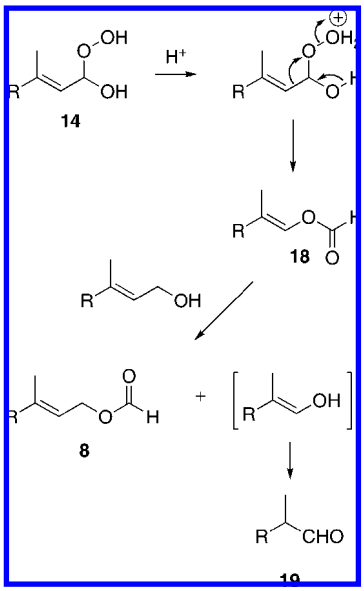

Figure 11. Formation of **8** through Baeyer−Villiger rearrangement and transesterification.

Finally, we shall discuss the formation of geranyl formate (**8**). This product differs from the other oxidation products in that it contains an additional carbon atom, which must have come from the fragmentation of another molecule of geraniol. We have not located any radical process leading to formates, but instead we speculate that it can be formed from perhydrate **14**, which can be formed either directly in the radical chain process as depicted in Figure 4 or by the reversible addition of hydrogen peroxide to either geranial (**3**) or neral (**4**), all of which are present in the autoxidation mixture. We note that **14** is reminiscent of the text-book intermediate in the Baeyer−Villiger reaction. Under acidic conditions, **14** is expected to fragment by cleavage of the O−O bond with simultaneous migration of the vinyl moiety, forming a vinyl formate (**18**). The latter has not been detected, but under the slightly acidic conditions of the autoxidation mixture, it would be expected to transesterify irreversibly with a geraniol molecule, whereupon the produced enol would tautomerize to C_9 aldehyde **19** (Figure 11).

A weakness of the current proposal is that aldehyde **19**, or indeed any C_9 products, has so far not been identified in the autoxidation mixture. However, geraniol is the only source of carbon in the experiment, and thus the only possible precursor for the formate moiety in **8**. In a separate experiment, a sample of authentic aldehyde **19** was added to geraniol and subjected to the normal oxidation procedure, as described previously.[7] The concentration of **19** slowly decreased and could, after a while, not be detected anymore. As negative evidence, this should not be taken as mechanistic

proof, but it at least indicates that the absence of **19** in the autoxidation mixture does not disprove the mechanism depicted in Figure 11. However, other Baeyer−Villiger-type mechanisms can also be proposed, since both hydrogen peroxide and hydroperoxides are present together with aldehydes in the autoxidation mixture.

Conclusions

The autoxidation products of the monoterpene geraniol (**2**) have been rationalized computationally by investigation of plausible radical chain reactions for a model system. Both propagation steps in the accepted mechanism, radical chain transfer and the addition of O_2, were found to be exergonic, in contrast to the recently investigated isomeric linalool system.[5] However, in addition to the normal chain transfer mechanism, the geraniol-derived peroxyl radicals can also undergo intramolecular hydrogen abstraction followed by fragmentation, liberating a hydroperoxyl radical as an alternative chain transfer agent. The latter process was found to be favored compared to the classical intermolecular hydrogen abstraction. Either process gives as a side product the observed hydrogen peroxide. Some of the located intermediates allow cis−trans isomerization of the original geraniol double bond, rationalizing the observation of both geranial and neral as oxidation products.

Secondary oxidation products like epoxides and formates were also considered, and plausible reaction pathways for the formation of both have been advanced, in the former case based on the oxidation of geraniol by a hydroperoxyl radical, in the latter case through a Baeyer−Villiger rearrangement of one of the oxidation intermediates.

Acknowledgment. The work of L.H. was financially supported by the Research Institute for Fragrance Materials, Inc. (RIFM). Support from the Swedish Research Council is gratefully acknowledged. The work is part of the platform Göteborg Science Center for Molecular Skin Research at the Faculty of Science, Göteborg University.

References

(1) Karlberg, A.-T.; Magnusson, K.; Nilsson, U. *Contact Dermatitis* **1992**, *26*, 332−340.

(2) Karlberg, A.-T.; Shao, L. P.; Nilsson, U.; Gäfvert, E.; Nilsson, J. L. G. *Arch. Derm. Res.* **1994**, *286*, 97−103.

(3) Sköld, M.; Börje, A.; Matura, M.; Karlberg, A.-T. *Contact Dermatitis* **2002**, *46*, 267−272.

(4) Sköld, M.; Börje, A.; Harambasic, E.; Karlberg, A.-T. *Chem. Res. Toxicol.* **2004**, *17*, 1697−1705.

(5) Bäcktorp, C.; Johnson Wass, J. R. T.; Panas, I.; Sköld, M.; Börje, A.; Nyman, G. *J. Phys. Chem. A* **2006**, *110*, 12204−12212.

(6) Wang, G.; Zhang, D.; Xu, X.; Zhou, J. *J. Phys. Chem. A* **2007**, *111*, 747−752.

(7) Hagvall, L.; Bäcktorp, C.; Svensson, S.; Nyman, G.; Börje A.; Karlberg, A.-T. *Chem. Res. Toxicol.* **2007**, *20*, 809−814.

(8) (a) Becke, A. D. *J. Chem. Phys.* **1993**, *98*, 5648. (b) Lee, C.; Yang, W.; Parr, R. G. *Phys. Rev. B: Condens. Matter Mater. Phys.* **1988**, *37*, 785. (c) Stephens, P. J.; Devlin, F. J.; Chabalowski, C. F.; Frisch, M. J. *J. Phys. Chem.* **1994**, *98*, 11623.

(9) Frisch, M. J.; Trucks, G. W.; Schlegel, H. B.; Scuseria, G. E.; Robb, M. A.; Cheeseman, J. R.; Montgomery, J. A., Jr.; Vreven, T.; Kudin, K. N.; Burant, J. C.; Millam, J. M.; Iyengar, S. S.; Tomasi, J.; Barone, V.; Mennucci, B.; Cossi, M.; Scalmani, G.; Rega, N.; Petersson, G. A.; Nakatsuji, H.; Hada, M.; Ehara, M.; Toyota, K.; Fukuda, R.; Hasegawa, J.; Ishida, M.; Nakajima, T.; Honda, Y.; Kitao, O.; Nakai, H.; Klene, M.; Li, X.; Knox, J. E.; Hratchian, H. P.; Cross, J. B.; Bakken, V.; Adamo, C.; Jaramillo, J.; Gomperts, R.; Stratmann, R. E.; Yazyev, O.; Austin, A. J.; Cammi, R.; Pomelli, C.; Ochterski, J. W.; Ayala, P. Y.; Morokuma, K.; Voth, G. A.; Salvador, P.; Dannenberg, J. J.; Zakrzewski, V. G.; Dapprich, S.; Daniels, A. D.; Strain, M. C.; Farkas, O.; Malick, D. K.; Rabuck, A. D.; Raghavachari, K.; Foresman, J. B.; Ortiz, J. V.; Cui, Q.; Baboul, A. G.; Clifford, S.; Cioslowski, J.; Stefanov, B. B.; Liu, G.; Liashenko, A.; Piskorz, P.; Komaromi, I.; Martin, R. L.; Fox, D. J.; Keith, T.; Al-Laham, M. A.; Peng, C. Y.; Nanayakkara, A.; Challacombe, M.; Gill, P. M. W.; Johnson, B.; Chen, W.; Wong, M. W.; Gonzalez, C.; and Pople, J. A. *Gaussian 03*, Revision B.05; Gaussian, Inc.: Wallingford, CT, 2004.

(10) (a) Olivella, S.; Solé, A. *J. Am. Chem. Soc.* **2003**, *125*, 10641−10650. (b) Pratt, D. A.; Mills, J. H.; Porter. N. A. *J. Am. Chem. Soc.* **2003**, *125*, 11827−11828.

(11) Rienstra-Kiracofe, J. C.; Allen, W. D.; Schaefer, H. F., III. *J. Phys. Chem. A* **2000**, *104*, 9823−9840.

CT7001495